


**Stability of a liquid film on inclined flexible substrates: Effect of the spontaneous odd viscosity**Beinan Jia and Yongjun Jian <sup>\*</sup>*School of Mathematical Science, Inner Mongolia University, Hohhot, Inner Mongolia 010021, People's Republic of China*

(Received 26 December 2022; revised 6 July 2023; accepted 8 September 2023; published 10 October 2023)

We report the stability of a falling incompressible odd viscosity fluid on flexible substrates when the time-reversal symmetry is broken. The flexible wall equation incorporates the contribution of odd viscosity, where the stress at an interface is determined by the viscosities of the adjacent fluids. The Orr-Sommerfeld (OS) equation is derived using the modified linear flexible wall equation taking the inertia, flexural rigidity, and spring stiffness effects of the elastic plate into account. Here, we solve the above eigenvalue problem using Chebyshev collocation methods to obtain the neutral curve in the  $k$ - $Re$  plane and the temporal growth rate under varying values of odd viscosity. There is an interesting finding that, for moderate Reynolds numbers, the presence of odd viscosity leads to an increase in instability when the stiffness coefficient  $A_K$  is small. However, as the value of the stiffness coefficient  $A_K$  rises, the effect of odd viscosity changes to suppress the onset of instability. Additionally, at higher Reynolds numbers and extremely small inclination angles, both shear and wall modes of falling film are observed. The results demonstrate that the unstable domain for the wall mode increases as the odd viscosity coefficient value rises, while an opposite trend occurs in the shear mode.

DOI: [10.1103/PhysRevE.108.045104](https://doi.org/10.1103/PhysRevE.108.045104)**I. INTRODUCTION**

The dynamics of waves formed on the free surface of falling films have several applications in geophysical, industrial, and technological settings [1–3]. Consequently, the studies of falling film instability have received considerable attention since the experimental work of Kapitza [4] and Binny [5]. Benjamin [6] and Yih [7] first studied theoretically a problem of hydrodynamic stability of falling films under the framework of the Orr-Sommerfeld boundary value problem. The important results of their investigation revealed that such instability occurs in the low Reynolds number regime once the Reynolds number surpasses its critical value  $Re_c = (5/4) \cot \theta$ , where  $\theta$  is the inclination angle. The inertia mechanism causes instability, whereas the longitudinal component of gravity adverts and steepens the wave, and surface tension stabilizes the film. The mechanism by which inertia destabilizes the film has been explained by either the shift in vorticity or the displacement of the interface [8,9]. In recent years, more research has been completed on falling film instability [10–12]. Lavalley *et al.* [13] investigated the linear stability of a falling liquid layer in combination with a gas phase moving down an inclined narrow channel. They concentrated on a specific region of parameter space with a modest inclination and very strong confinement, where they discovered the gas firmly stabilizes the film. Zhou *et al.* [14] investigated the dynamics of annular viscoelastic films flowing down a flexible tube. They discovered that the interfacial capillary ripples are frequently stimulated by the tube's rigidity. Although it weakens the interfacial capillary ripples, the viscoelasticity of the fluid increases the dispersion of interfacial waves.

Over the last few decades, the theory of viscous flow interacting with compliant walls has been developed significantly. Kramer [15] performed ground-breaking experiments in the water by towing a dolphin-shaped device wrapped in viscoelastic materials of varied compliance. The author demonstrates that the compliant coating reduces drag significantly. Later, a theoretical study on the effects of a flexible boundary on hydrodynamic stability is presented by Benjamin [16]. In this context, Carpenter, and Garrad [17] considered the hydrodynamic stability of flows over Kramer-type compliant surfaces, and provided a possible explanation based upon Kramer's empirical observation of an optimum substrate viscosity. Halpern and Grotberg [18] analyzed the dynamics of a thin film of Newtonian fluid coating the inner surface of an elastic circular tube. The most common investigations can be divided into two physical models for the elastic substrate: Carpenter and Garrad's [17] spring-backed plate membrane concept, as well as an elastic solid substrate of finite thickness over which the liquid film falls. Several notable references provide details on viscous flow interacting with compliant barriers [19–23].

Recently, Alexander *et al.* [24] used analytical and computational tools to examine the linear stability of a liquid film falling down an inclined flexible plane under the effect of gravity. They employed the flexible substrate model proposed by Carpenter and Garrad [17] and presented a modified version of the linear wall equation, which incorporates the viscous traction of the fluid that was previously omitted in [17]. They kept inertia, damping, tension, flexural rigidity, and stiffness effects in wall equation and calculated their effects on falling film stability. Later, Samanta [25] extended this research to investigate the linear stability of a fluid flowing down a compliant substrate in the presence of insoluble surfactants when an external streamwise applied shear stress operates

<sup>\*</sup>Corresponding author: [jianyuj@imu.edu.cn](mailto:jianyuj@imu.edu.cn)

at the fluid surface. By modeling the walls as spring-backed deformable plates with a damping mechanism, Lebbal *et al.* [26] explored the linear stability problem of a fluid interacting with a compliant channel. To find the most physically applicable control settings, they also performed a dimensional analysis. Subsequently, Lebbal *et al.* [27] also examined the linear dynamics of perturbations arising in an infinite channel with compliant walls under pulsatile flow circumstances. For Womersley-type pulsating base flows, two-dimensional modal disturbances are taken into account, and wall motion is only permitted in the normal direction.

The researches on viscous flow interacting with compliant walls noted above, however, have only looked at fluids with even (standard) viscosities. In other words, the impact of unusual viscosity was disregarded. By proving that the viscosity tensor in a general classical fluid can have a nonzero odd part that results in a dissipationless linear response coefficient known as the Hall or odd viscosity when time-reversal symmetries are broken spontaneously, as a result of an external magnetic field, or as a result of rotation, Avron [28] made a ground-breaking discovery. Odd viscosity had previously been hypothesized in relation to plasmas, but it has only recently drawn interest from researchers in the contexts of swimming strategies [29], and incompressible fluids [30,31]. Banerjee *et al.* [32] investigated the hydrodynamics of a spin fluid made up of colloidal or spin particles. They demonstrated how nonlinear hydrodynamic equations with rotating degrees of freedom lead to odd viscosity. Odd viscosity effects are widely seen in granular, biological, colloidal, and other systems in natural settings where the time-reversal symmetry of a classical liquid is violated [33–35]. The role of odd viscosity in the investigation of hydrodynamic instability of thin fluid film was introduced by Kirkinis and Andreev [36]. They examined the impact of odd viscosity on thermocapillary instability among viscous thin liquid layers using the long-wave approximation approach. They demonstrated that odd viscosity can stabilize the thin liquid film by suppressing thermocapillary instability within a specific range of ratios of odd to even viscosity coefficients.

Recently, Soni *et al.* [37] experimentally demonstrated the existence of odd viscosity by using spectral analysis. They observed the production of a two-dimensional chiral liquid that was cohesive and studied its flows using millions of spinning colloidal magnets and discovered that dissipative viscous “edge pumping,” which has no analog in ordinary fluids, is a crucial and general process of chiral hydrodynamics, causing unidirectional surface waves and instabilities. In the presence of a uniform external electric field, Bao and Jian [38] investigated how the unusual viscosity of a Newtonian fluid affects the instability of a thin film moving down an inclined plane. With the aid of the lubrication approximation, a nonlinear evolution equation of the free surface involving odd viscosity effect was derived. Analyses of linear and weakly nonlinear stability indicate that odd viscosity has the stabilizing effect, whereas the electric field destabilizes. Zhao and Jian [39,40] investigated the impact of odd viscosity on the stability of a thin film falling in the presence of an electromagnetic field, considering both Newtonian and viscoelastic fluids using long wave approximation theory. The influence of odd viscosity on the Rayleigh-Taylor instability of a thin Newtonian liquid

film with broken time-reversal symmetry, as it flows down an inclined and uniformly heated substrate, was discussed by Jia and Jian [41]. In regard to a fluid experiencing an influence of odd viscosity, Samanta [42] studied the linear and nonlinear wave dynamics of a falling incompressible viscous fluid. Chu *et al.* [43] used both linear Floquet theory and nonlinear lubrication theory based on the weighted residual model to study the impact of the odd viscosity on the classic Faraday instability of thin liquid films in infinite horizontal plates. Chattopadhyay *et al.* [44] studied the role of odd viscosity on falling films over compliant substrates and utilized the long wave theory to derive equations that couple the film thickness and the compliant substrate. The results showed that odd viscosity suppresses the instability of falling films. However, in their work, the effects of inertia, flexural rigidity, and spring stiffness of the elastic plate were disregarded. These details spur us on to thoroughly research the thin film instability for incompressible fluids with broken time-reversal symmetry.

In this study, we utilize the flexible wall model proposed by Alexander *et al.* [24] and take into account the stress at an interface involving the effect of the odd viscosity in adjacent fluids. In fact, if the substrate is assumed sufficiently thin, the impact of bending stress and inertia on the substrate cannot be neglected. The bending stress is expressed by fourth order derivative of the wall deformation with respect to horizontal coordinate  $x$ . Therefore, it is difficult to obtain the nonlinear evolution equation of free surface by long wave theory or weighted residual method. Our objective is to comprehensively investigate the impacts of spontaneous odd viscosity, inertia, flexural rigidity, and spring stiffness of the flexible substrate on the stability of a falling liquid film. The method adopted in present work is regular mode expansion of the perturbation imposed upon base state. The Orr-Sommerfeld (OS) eigenvalue problem is obtained and the Chebyshev collocation method is utilized to illustrate temporal growth rate and neutral stable curve for different related parameters. A vital discrepancy between our results and those obtained by Chattopadhyay *et al.* [44] is that the effect of odd viscosity is not monotonous and it depends on the value of spring stiffness coefficient  $A_K$ . For moderate Reynolds numbers, odd viscosity enlarges the unstable domain when  $A_K$  is small. However, as the value of  $A_K$  increases, the influence of odd viscosity will suppress the onset of instability.

## II. MATHEMATICAL MODEL

As shown in Fig. 1, we consider an incompressible odd-viscosity fluid flowing down a flexible and inclined surface at an angle  $\alpha$  with the horizontal direction. A two-dimensional coordinate system  $(x, y)$  is introduced, in which the  $x$  and  $y$  coordinates are in the directions along and normal to the undeformable elastic plate, respectively. Therefore, the thickness of the interfacial surface at time  $t$  is given by  $h(x, t)$ , the velocity of fluid is  $\bar{u} = (u, v)$ , and the instantaneous substrate deflection from its equilibrium position is denoted by  $y = \eta(x, t)$ .

We consider a classical Newtonian liquid with broken time-reversal symmetry and an odd or Hall viscosity coefficient. Therefore, the viscosity contains both even  $\mu^e$  and odd  $\mu^o$  viscosity coefficients. In a liquid with broken

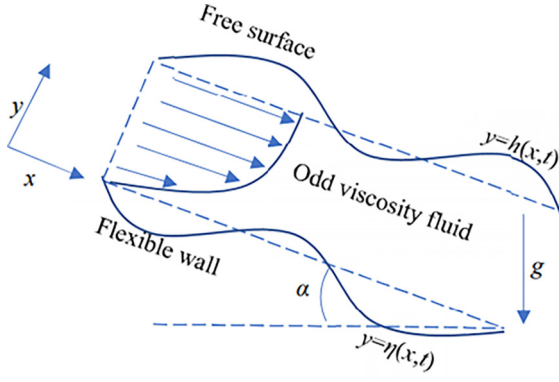


FIG. 1. Schematic diagram of an odd-viscosity fluid flowing down a flexible and inclined substrate, where  $g$  is the acceleration of gravity.

time-reversal symmetry, the Cauchy stress tensor  $\boldsymbol{\tau}$  consists of two parts [38–43],

$$\boldsymbol{\tau} = \boldsymbol{\tau}^e + \boldsymbol{\tau}^o, \quad (1)$$

$$\tau_{ij}^e = -p\delta_{ij} + \mu^e \left( \frac{\partial u_i}{\partial x_j} + \frac{\partial u_j}{\partial x_i} \right), \quad (2)$$

$$\begin{aligned} \tau_{ij}^o = & -\mu^o(\delta_{i1}\delta_{j1} - \delta_{i2}\delta_{j2}) \left( \frac{\partial u_1}{\partial x_2} + \frac{\partial u_2}{\partial x_1} \right) \\ & + \mu^o(\delta_{i1}\delta_{j2} - \delta_{i2}\delta_{j1}) \left( \frac{\partial u_1}{\partial x_1} - \frac{\partial u_2}{\partial x_2} \right), \end{aligned} \quad (3)$$

where  $\boldsymbol{\tau}^o$  is the odd part of the Cauchy stress tensor, which arises in the presence of time-reversal symmetry-breaking, and  $\boldsymbol{\tau}^e$  is the general even part of the Cauchy stress tensor.

The flowing governing equations are the incompressible Navier-Stokes equations,

$$\nabla \cdot \vec{u} = 0, \quad (4)$$

$$\rho \frac{D\vec{u}}{Dt} = \nabla \cdot \boldsymbol{\tau} + \vec{f}, \quad (5)$$

where  $\vec{f}$  is the force of gravity acting on the odd-viscosity fluid. Using Eqs. (1)–(5), we can obtain the flowing governing equations for the odd viscosity fluid:

$$u_x + v_y = 0, \quad (6)$$

$$\begin{aligned} u_t + uu_x + vv_y = & -\frac{1}{\rho}p_x + g \sin \alpha + \frac{\mu^e}{\rho}(u_{xx} + u_{yy}) \\ & - \frac{\mu^o}{\rho}(v_{xx} + v_{yy}), \end{aligned} \quad (7)$$

$$\begin{aligned} v_t + uv_x + vv_y = & -\frac{1}{\rho}p_y - g \cos \alpha \\ & + \frac{\mu^e}{\rho}(v_{xx} + v_{yy}) + \frac{\mu^o}{\rho}(u_{xx} + u_{yy}) \end{aligned} \quad (8)$$

where the subscripts denote partial derivatives.

The boundary conditions at the free interface  $y = h(x, t)$  are the balance of tangential, normal stresses:

$$\vec{n} \cdot \boldsymbol{\tau} \cdot \vec{n} = -\kappa \cdot \sigma, \quad \vec{n} \cdot \boldsymbol{\tau} \cdot \vec{t} = 0, \quad (9)$$

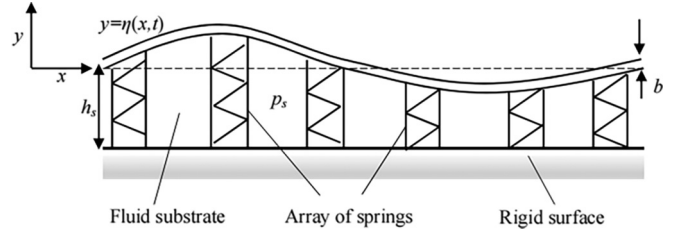


FIG. 2. Schematic diagram of a flexible substrate. The elastic plate is supported by an array of springs and has a thickness of  $b$  and  $h_s$  is the equilibrium height of the substrate fluid.

where  $\sigma$  is the surface tension of the liquid-air interface,  $\kappa = \nabla \cdot \vec{n}$ , combining (1)–(3) and (9), the boundary conditions can be written,

$$\begin{aligned} -p + \frac{1}{1+h_x^2} [2\mu^e(h_x^2 - 1)u_x - 2\mu^e h_x(u_y + v_x) \\ + \mu^o(u_y + v_x)(1 - h_x^2) - 2\mu^o h_x(u_x - v_y)] \\ = \frac{\sigma h_{xx}}{(1+h_x^2)^{3/2}}, \end{aligned} \quad (10)$$

$$\begin{aligned} \frac{1}{1+h_x^2} [\mu^e(1 - h_x^2)(u_y + v_x) + 2\mu^e h_x(v_y - u_x) \\ + 2\mu^o h_x(u_y + v_x) - \mu^o(1 - h_x^2)(u_x - v_y)] = 0, \end{aligned} \quad (11)$$

and kinematic boundary condition is

$$h_t + uh_x - v = 0, \quad \text{at } y = h(x, t), \quad (12)$$

where  $h_x$  indicates the associated partial derivatives.

The physical model of a flexible wall is shown schematically in Fig. 2. It consists of an elastic plate that is supported by an array of springs above a rigid surface. The cavity between the elastic plate and the rigid substrate is filled with a viscous fluid, which is referred to as the substrate fluid. Furthermore, a fluid substrate that supports the plate typically has a different density and viscosity from the main flow. It is assumed that the motion of the substrate fluid is barely impacted by the springs' presence. According to the work of Alexander *et al.* [24], we consider the flexible model:

$$\begin{aligned} \rho_w b \mathbf{X}_{tt} \cdot \vec{n} + D(e_y \cdot \mathbf{X}_t)(e_y \cdot \vec{n}) - (T \mathbf{X}_s)_s \cdot \vec{n} \\ + B \mathbf{X}_{ssss} \cdot \vec{n} + K(e_y \cdot \mathbf{X})(e_y \cdot \vec{n}) \\ = \vec{n} \cdot \boldsymbol{\tau} \cdot \vec{n}|_{x=X} + p_s, \end{aligned} \quad (13)$$

where  $\rho_w$  is the density of the plate material,  $b$  is the thickness of the elastic plate,  $D$  is the damping coefficient,  $B$  is the flexural rigidity of the elastic plate,  $T$  is the longitudinal tension per unit width,  $K$  is the spring stiffness,  $p_s$  is the pressure of the substrate fluid, and  $e_y$  is the unit vector in the  $y$  direction.  $\mathbf{X}(s, t) = [X(s, t), Y(s, t)]$  is the parameter coordinate and  $s$  denotes the arc length. The unit tangent and normal to the plate can be written as

$$\vec{n} = \frac{1}{\sqrt{1+\eta_x^2}}(-\eta_x, 1), \quad \vec{t} = \frac{1}{\sqrt{1+\eta_x^2}}(1, \eta_x). \quad (14)$$

In practice, the flexural rigidity  $B$  and the damping coefficient  $D$  are not independent wall parameters.

Based on the study of Alexander *et al.* [24], the flexural rigidity and damping coefficient are respectively defined as

$$B = \frac{Eb^3}{12(1-\nu^2)}, \quad D = 2\zeta\sqrt{K\rho_w b}, \quad (15)$$

where  $E$  is Young's modulus,  $\nu$  is the Poisson ratio of the elastic material, and  $\zeta$  is the damping ratio.

In our study, the odd viscosity should be contemplated on the right side of the flexible model. Using the odd viscosity Cauchy stress tensor  $\boldsymbol{\tau}$ , the condition of normal stresses is derived at the flexible wall surface,

$$\begin{aligned} \vec{n} \cdot \boldsymbol{\tau} \cdot \vec{n}|_{x=X} = & -P + \frac{1}{1+\eta_x^2} [2\mu^e(\eta_x^2 - 1)u_x \\ & - 2\mu^e\eta_x(u_y + v_x) + \mu^o(u_y + v_x)(1 - \eta_x^2) \\ & - 2\mu^o\eta_x(u_x - v_y)]. \end{aligned} \quad (16)$$

We suppose that the amplitude of wall  $\eta$  will be much smaller than the film thickness. Thus,  $\eta_x \ll 1$ ,  $\eta_x^2$  can be ignored:

$$\begin{aligned} \vec{n} \cdot \boldsymbol{\tau} \cdot \vec{n}|_{x=X} = & -P + 2\mu^e[v_y - \eta_x(u_y + v_x)] \\ & + \mu^o[(u_y + v_x) - 2\eta_x(u_x - v_y)]. \end{aligned} \quad (17)$$

The simplified detailed process on the left-hand side of Eq. (13) is given in the paper of Alexander *et al.* [24]. Finally, we obtain the linear soft wall equation which takes into account the stress at an interface involving the effect of the odd viscosity in adjacent fluids:

$$\begin{aligned} \rho_w b \eta_{tt} + D \eta_t - T \eta_{xx} + B \eta_{xxxx} + K \eta \\ = p_s - p + 2\mu^e[v_y - \eta_x(u_y + v_x)] \\ + \mu^o[(u_y + v_x) - 2\eta_x(u_x - v_y)]. \end{aligned} \quad (18)$$

The modified equation reduces to the one obtained by Alexander *et al.* [24] when the odd viscosity coefficient  $\mu^o$  is equal to zero.

In addition, the linear wall Eq. (18) is subject to the following no-slip and kinematic conditions at the compliant substrate [25],

$$u = 0, \quad v = \eta_t, \quad \text{at } y = 0. \quad (19)$$

We use the following set of scales to normalize the above governing system:

$$\begin{aligned} (u, v) = u_0(u^*, v^*), \quad (x, y, h) = h_0(x^*, y^*, h^*), \\ p = \frac{\mu^e u_0}{h_0} p^*, \quad t = \frac{h_0}{u_0} t^*, \quad u_0 = \frac{\rho g h_0^2 \sin \alpha}{2\mu^e}, \\ [5pt] \mu = \frac{\mu^o}{\mu^e}, \quad \text{Re} = \frac{\rho u_0 h_0}{\mu^e}, \quad \eta^* = \frac{\eta}{h_0}, \quad S = \frac{\sigma}{\mu^e u_0}, \end{aligned} \quad (20)$$

where  $u_0$  is given by the balance between the  $x$  component of gravity and the viscous force [25]. Using the dimensionless variables above, the governing equations reduce to the

following form, and the star in the nondimensional is dropped in the following discussion:

$$u_x + v_y = 0, \quad (21)$$

$$\text{Re}(u_t + uu_x + vv_y) = 2 + u_{xx} + u_{yy} - \mu(v_{xx} + v_{yy}) - p_x, \quad (22)$$

$$\begin{aligned} \text{Re}(v_t + uv_x + vv_y) = & -2 \cot \alpha + v_{xx} + v_{yy} \\ & + \mu(u_{xx} + u_{yy}) - p_y. \end{aligned} \quad (23)$$

At  $y = h(x, t)$ , the dimensionless stress tensor and the kinematic boundary conditions are

$$\begin{aligned} -p + \frac{1}{1+h_x^2} [2(h_x^2 - 1)u_x - 2h_x(u_y + v_x) \\ + \mu(u_y + v_x)(1 - h_x^2) - 2\mu h_x(u_x - v_y)] \\ = \frac{h_{xx}}{(1+h_x^2)^{3/2}} S, \end{aligned} \quad (24)$$

$$\begin{aligned} \frac{1}{1+h_x^2} [(1 - h_x^2)(u_y + v_x) + 2h_x(v_y - u_x) + 2\mu h_x(u_y + v_x) \\ - \mu(1 - h_x^2)(u_x - v_y)] = 0, \end{aligned} \quad (25)$$

$$h_t + uh_x - v = 0, \quad (26)$$

The conditions at soft wall  $y = \eta(x, t)$  become

$$u = 0, \quad v = \eta_t, \quad (27)$$

$$\begin{aligned} A_I \eta_{tt} + A_D \eta_t - A_T \eta_{xx} + A_B \eta_{xxxx} + A_K \eta \\ = p_s - p + 2[v_y - \eta_x(u_y - v_x)] \\ + \mu[(u_y + v_x) - 2\eta_x(u_y - v_x)], \end{aligned} \quad (28)$$

where  $A_I = \rho_w u_0 b / \mu^e$ ,  $A_D = Dh_0 / \mu^e$ ,  $A_T = T / \mu^e u_0$ ,  $A_B = B / h_0^2 \mu^e u_0$ , and  $A_K = Kh_0^2 / \mu^e u_0$  indicate the ratios of wall inertia, damping, wall tension, flexural rigidity, and spring stiffness to viscous stress, respectively.

We consider the base flow is a unidirectional parallel flow with a constant fluid layer height and without compliant substrate deformation  $\eta = 0$ . Therefore, the simplified governing equations and boundary conditions for the base flow are

$$U_{yy} = -2, \quad (29)$$

$$\mu U_{yy} = 2 \cot \alpha + P_y. \quad (30)$$

$$U = 0, \quad P = p_s, \quad \text{at } y = 0. \quad (31)$$

$$\mu U_y = 0, \quad P = \mu U_y, \quad \text{at } y = 1. \quad (32)$$

The exact solution of the base flow equations in nondimensional form (29)–(32) is given by

$$\begin{aligned} U = y(2 - y), \quad v = 0, \quad h = 1, \quad \eta = 0, \\ P = (\mu + \cos \alpha)(1 - y), \quad p_s = \mu + \cos \alpha. \end{aligned} \quad (33)$$

### III. LINEAR STABILITY ANALYSIS

To study the linear stability analysis, we shall first derive the perturbation equations for the infinitesimal disturbance. To

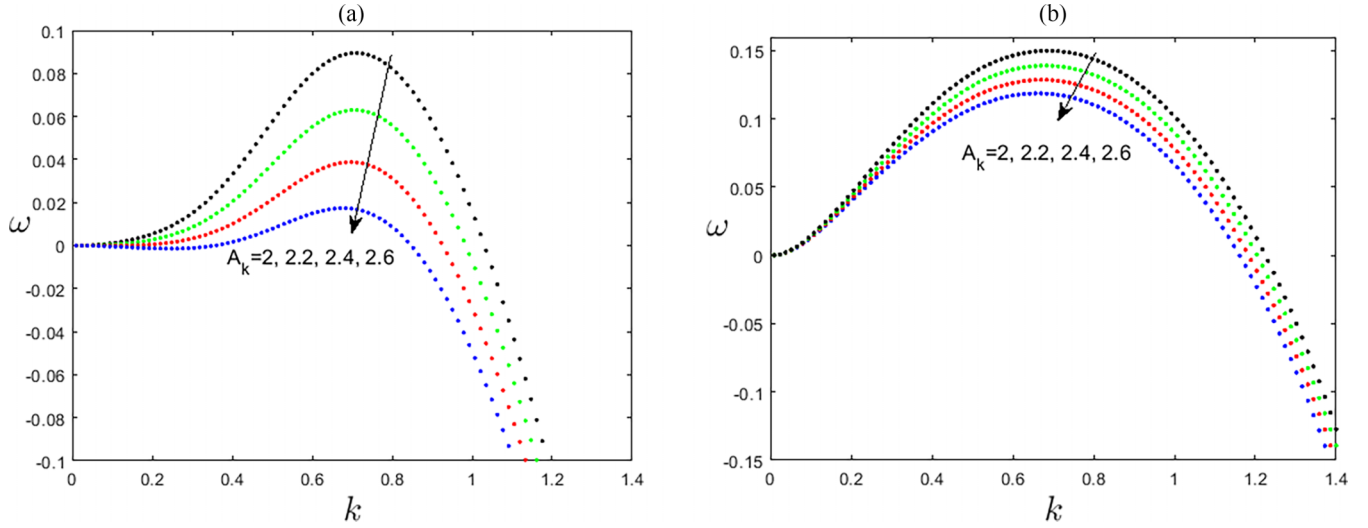


FIG. 3. The temporal growth rate  $\omega$  with the different values of  $A_k$ , when  $A_I = 1$ ,  $A_B = 1$ ,  $A_D = 1$ ,  $A_T = 1$ ,  $S = 1$ , and  $\alpha = \pi/4$ . (a)  $\text{Re} = 0.2$ . (b)  $\text{Re} = 3$ .

this end, an infinitesimal disturbance is applied to the base flow. This fact is mathematically expressed by the following flow variable decomposition:

$$u(x, y, t) = U(y) + u'(x, y, t), \quad (34a)$$

$$v(x, y, t) = v'(x, y, t), \quad (34b)$$

$$p(x, y, t) = P(y) + p'(x, y, t), \quad (34c)$$

$$h(x, t) = 1 + h'(x, t), \quad (34d)$$

$$\eta(x, t) = \eta'(x, t), \quad (34e)$$

where the variables with primes represent the perturbation velocity components, perturbation pressure, and perturbation surface deformation, respectively. By substituting (34) into Eqs. (21)–(28), the linearized forms of perturbation equations and boundary conditions are

$$u'_x + v'_y = 0, \quad (35)$$

$$\text{Re}(u'_t + Uu'_x + v'U_y) = u'_{xx} + u'_{yy} - \mu(v'_{xx} + v'_{yy}) - p'_x, \quad (36)$$

$$\text{Re}(v'_t + Uv'_x) = v'_{xx} + v'_{yy} + \mu(u'_{xx} + u'_{yy}) - p'_y. \quad (37)$$

At  $y = 1$ , the balance of tangential, normal stresses, and kinematic boundary conditions become

$$-p' - 2u'_x + 2h'(\mu + \cot \alpha) + \mu(u'_y + h'U_{yy} + v'_x) = h'_{xx}S, \quad (38)$$

$$u'_y + v'_x - 2h' + \mu(u'_x - v'_y) = 0, \quad (39)$$

$$h'_t + h'_x - v' = 0. \quad (40)$$

At  $y = 0$ , the boundary conditions of the interface for the liquid film and flexible wall are written

$$u' = -2\eta', \quad v' = \eta'_t, \quad (41)$$

$$A_I \eta'_{tt} + A_D \eta'_t - A_T \eta'_{xx} + A_B \eta'_{xxxx} + A_K \eta' - 2(\mu + \cot \alpha) \eta' = -p' + 2(v'_y - 2\eta'_x) + \mu(u'_y + v'_x). \quad (42)$$

Then, we use the normal modes of the following form to substitute the solution of the perturbation Eqs. (35)–(42),

$$(u', v', p', h', \eta') = [\tilde{u}(y), \tilde{v}(y), \tilde{p}(y), \tilde{h}, \tilde{\eta}] e^{ik(x-ct)} + \text{c.c.}, \quad (43)$$

where c.c. represents the complex conjugate and the variables with tildes representing the amplitudes of perturbation variables,  $k$  is the real wave number,  $c = c_r + ic_i$  is the complex propagating speed, and  $\omega = kc_i$  is growth rate. Besides, we introduce the perturbation stream function

$$\psi'_y = u', \quad -\psi'_x = v', \quad (44)$$

and the normal modes are

$$\psi'(x, y, t) = \tilde{\psi}(y) e^{ik(x-ct)}, \quad \tilde{u} = \tilde{\psi}_y, \quad \tilde{v} = -ik\tilde{\psi}. \quad (45)$$

Combining Eqs. (31)–(42) and eliminating the pressure terms, one can obtain the OS eigenvalue problem for the falling viscous fluid with broken time-reversal symmetry:

$$\left( \frac{d^2}{dy^2} - k^2 \right)^2 \tilde{\psi} - ik \text{Re}(U - c) \left( \frac{d^2}{dy^2} - k^2 \right) \tilde{\psi} + ik \text{Re} U_{yy} \tilde{\psi} = 0. \quad (46)$$

The boundary conditions at  $y = 1$  are

$$\tilde{\psi}_{yy} + \left( k^2 + \frac{2}{1-c} \right) \tilde{\psi} + \mu(ik\tilde{\psi}_{yy} + ik\tilde{\psi}_y) = 0, \quad (47)$$

$$i\tilde{\psi}_{yyy} + [k \text{Re}(1-c) - 3ik^2] \tilde{\psi}_y - \left( \frac{2k \cot \alpha + Sk^3}{1-c} - \mu k^3 \right) \tilde{\psi} = 0. \quad (48)$$

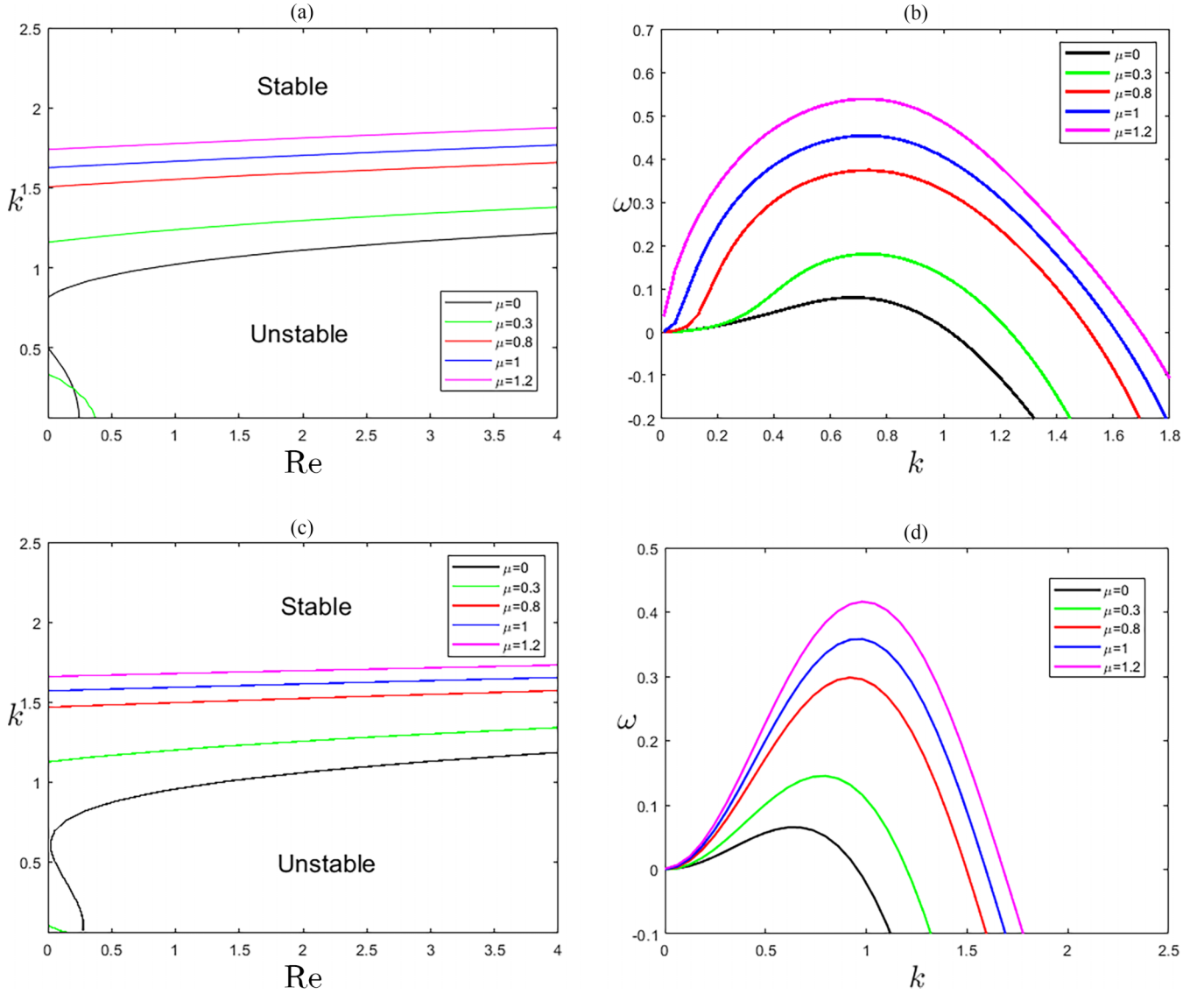


FIG. 4. (a), (c) The neutral curve in the  $k$ -Re plane with the different values of viscosity ratio  $\mu$ , when  $A_K = 2.5$ ,  $A_I = A_D = A_T = A_B = 1$ ,  $\alpha = \pi/4$ ,  $S = 1$  and 500. (b), (d) The temporal growth rate  $\omega$  with the different values of viscosity ratio  $\mu$ , when  $A_K = 2.5$ ,  $A_I = A_D = A_T = A_B = \text{Re} = 1$ ,  $\alpha = \pi/4$ ,  $S = 1$ , and 500.

The boundary conditions at  $y = 0$  are

$$\tilde{\psi}_y = -\frac{2}{c}\tilde{\psi}, \quad (49)$$

$$\begin{aligned} & [-k^2 c A_I - i k c A_D + k^2 A_T + k^4 A_B + A_K \\ & - 2(\mu + \cot \alpha) - 2c\mu k^2] \tilde{\psi} \\ & = -\frac{c}{ik} \tilde{\psi}_{yyy} + 2ik \tilde{\psi}. \end{aligned} \quad (50)$$

#### IV. STABILITY ANALYSIS IN THE ARBITRARY WAVE NUMBER

##### A. Numerical methods

To analyze the stability of the liquid film flow for arbitrary wave number, we use Chebyshev collocation methods to resolve the linearized forms of perturbation equations. The universal code of the numerical methods is developed by Han

*et al.*, from Beihang University [45]. The code is based on MATLAB for solving hydrodynamic stability problems.

We choose the parameter values as given in Alexander *et al.* [24], to validate the numerical code. The growth rates are presented in Figs. 3(a) and 3(b) for  $\text{Re} = 0.2$  and  $\text{Re} = 3$ , respectively, with the stiffness  $A_K$  varying between 2.0 and 2.6 when odd viscosity  $\mu = 0$ . The temporal growth rate enhances with the decreasing value of  $A_K$ . Hence, the increasing value of  $A_K$  has a stabilizing effect on the surface mode. It shows an excellent agreement between the current results and the results of Alexander *et al.* [24].

##### B. Numerical results at moderate Reynolds number regime

To analyze the effect of odd viscosity, the viscosity ratio  $\mu$  is changed in the numerical simulation. The neutral stability curve in the  $k$ -Re plane and the temporal growth rate  $\omega$  at  $\text{Re} = 1$  are given in Figs. 4(a) and 4(b), respectively.

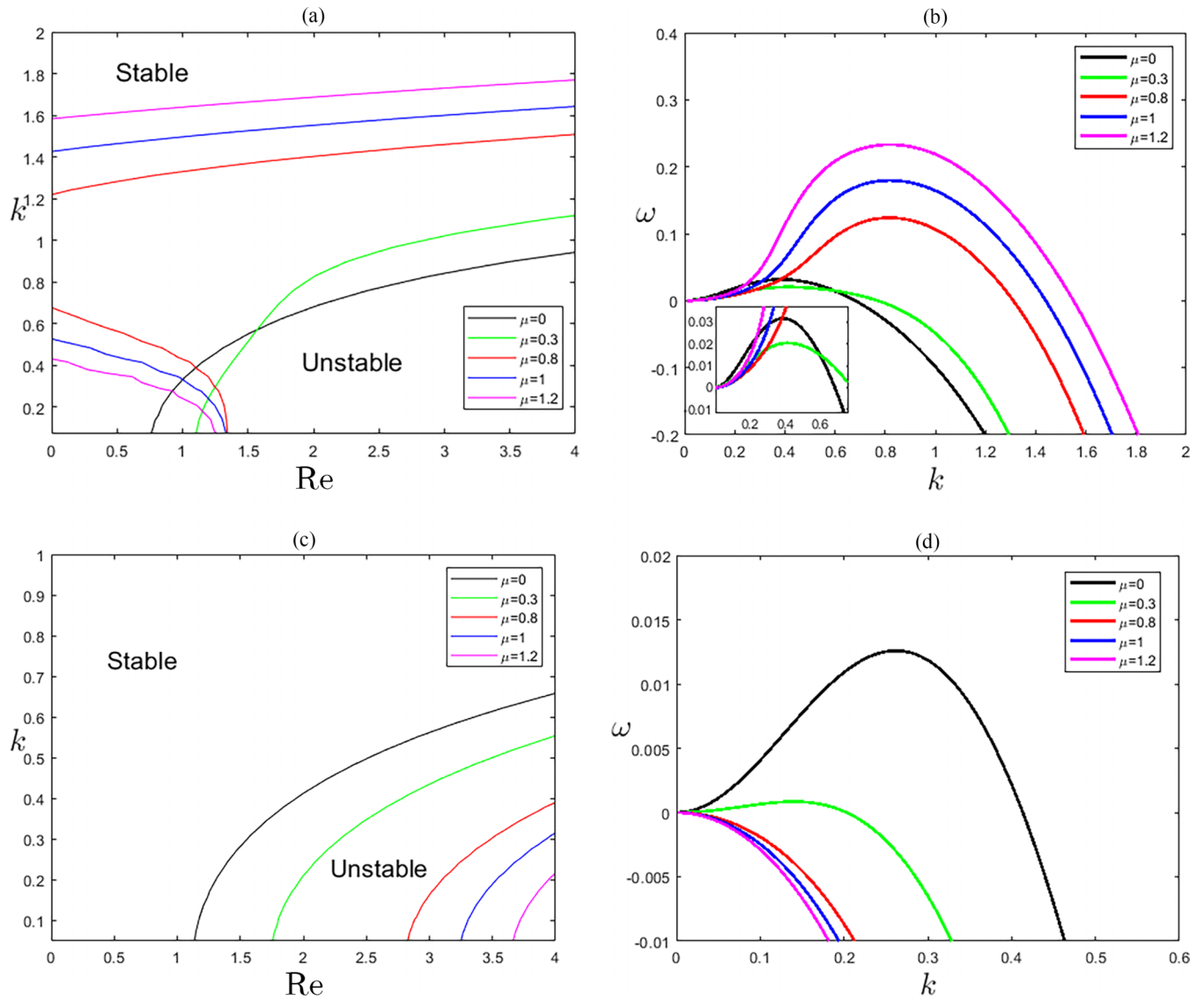


FIG. 5. The neutral curve in the  $k$ - $Re$  plane and temporal growth rate  $\omega$  with the different values of viscosity ratio  $\mu$ , when  $A_I = A_D = A_T = A_B = S = 1$ , and  $\alpha = \pi/4$ . (a)  $A_K = 5$ . (b)  $A_K = 5$ ,  $Re = 2$ . (c)  $A_K = 20$ . (d)  $A_K = 20$ ,  $Re = 2$ .

Figure 4(a) illustrates the unstable domain magnifies with the increasing value of  $\mu$ . Thus, the effect of odd viscosity enhances the instability of liquid film. It can be found that the primary instability emerges in the finite wave-number regime instead of the long wave regime at the odd viscosity ratio  $\mu = 0$ , which agrees with the result in Samanta [42]. Further, this phenomenon gradually disappears, when the rate of viscosity increases. That means that the flow of the liquid film is stable in the long wave regime when the odd viscosity coefficient  $\mu$  is small for low values of  $Re$ . The short-wave instability at  $Re = 0$  exists also for  $\mu = 0$ , and this result has been reported previously, e.g., in Alexander *et al.* [24]. However, due to the higher odd viscosity ratio  $\mu$ , the instability produced persists even at zero Reynolds number, which means an inertialess instability was induced in the finite wave-number regime.

Figure 4(b) shows the temporal growth rates  $\omega$  for different values of the viscosity ratio  $\mu$ . It is clear that the representative growth rate increases as the odd viscosity coefficient  $\mu$  increases. Therefore, the above result further confirms that

the instability of the liquid film is enhanced by the effect of odd viscosity. Furthermore, for a realistic value of parameter  $S = 500$ , Figs. 4(c) and 4(d) illustrate the neutral curve and temporal growth rate. Figures 4(c) and 4(d) also demonstrate that the flow becomes more unstable as the rate of viscosity increases, which is consistent with the findings in Figs. 4(a) and 4(b). Comparing Figs. 4(a) and 4(c), it is easy to find that the unstable regime decreases for the value of  $S = 500$ .

Figures 5(a) and 5(c) exhibit the neutral curve in the  $k$ - $Re$  plane when the viscosity ratio  $\mu$  alters and stiffness coefficient  $A_K = 5$  and 20, respectively. In Fig. 5(a), it is found that the critical  $Re$  is larger than that in Fig. 4(a) due to a larger  $A_K$ . It is demonstrated that the flow for arbitrary wave number is stable when  $Re$  is close to zero, at  $\mu = 0$  and 0.3. However, the unstable domain emerges in the finite wave-number regime when the odd viscosity coefficient increases, even if the Reynolds number is zero. Corresponding growth rates  $\omega$  are raised by the amplifying values of viscosity ratio  $\mu$ , as in Fig. 5(b). This result further proves that the odd viscosity

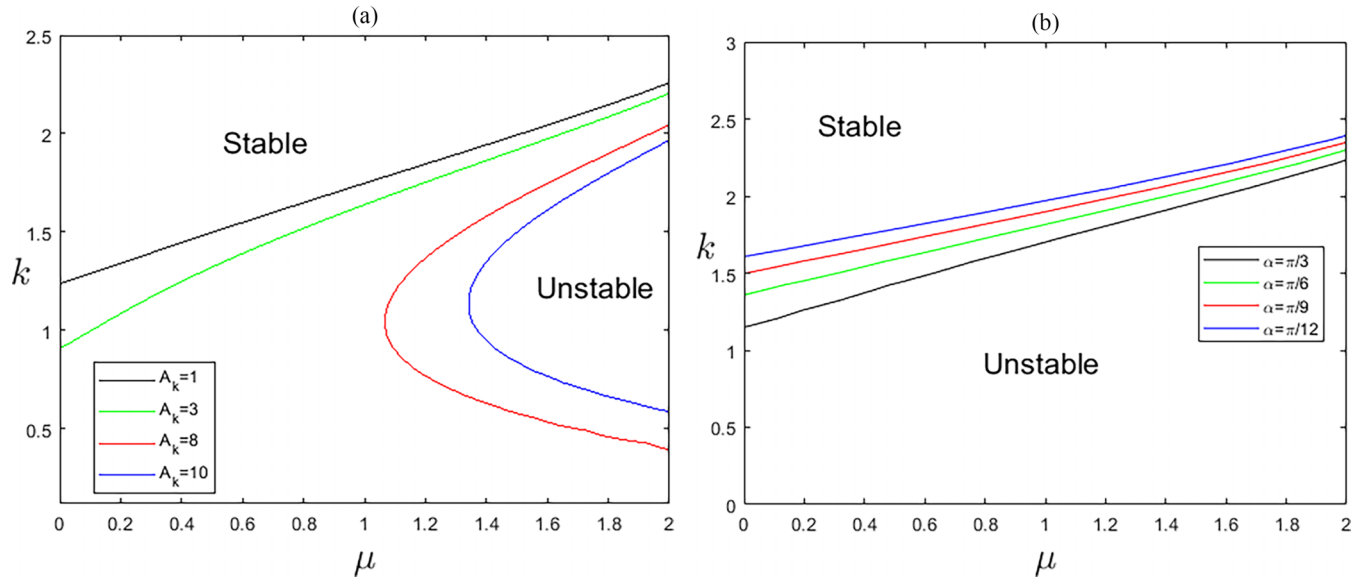


FIG. 6. (a) The neutral curve in the  $k$ - $\mu$  plane with the different values of  $A_K$ , when  $Re = A_I = A_D = A_T = A_B = 1$ , and  $\alpha = \pi/4$ . (b) The neutral curve in the  $k$ - $\mu$  plane with the different values of  $\alpha$ , when  $Re = A_I = A_D = A_T = A_B = 1$ , and  $A_K = 1.5$ .

effect enhances the instability of the flowing liquid film on the flexible substrate. Moreover, it is important to note that the unstable domain for the liquid film decreases with an increase in  $\mu$ , at  $\mu = 0.3$  and  $0$ , when the Reynolds numbers and wave number are small, as in Fig. 5(a). To strengthen this consequence, we observe that the temporal growth rate  $\omega$  varies with the increasing odd viscosity ratio  $\mu$ . The subimage of Fig. 5(b) shows that the temporal growth rate  $\omega$  reduces as the odd viscosity ratio  $\mu$  increases, in the long wave regime. Apparently, an opposite result can be found for a larger value of stiffness  $A_K$ . Therefore, we choose the larger  $A_K = 20$  to observe the variation of unstable domain with viscosity ratio  $\mu$  in Fig. 5(c). It should be noted that the unstable domain in the finite wave-number regime decreases with the increasing

value of  $\mu$ . It is demonstrated that when the stiffness of the flexible wall is high, the odd viscosity suppresses instability of the flow at moderate Reynolds numbers. Furthermore, Fig. 5(d) also displays the suppressing effect of odd viscosity on temporal growth rate  $\omega$ . Combined with the results of Figs. 4 and 5, we can infer that as the stiffness  $A_K$  increases, the effect of odd viscosity on instability is not monotonous. As discussed by Alexander *et al.* [24], the flexible substrate behaves gradually like a rigid substrate with increasing values of the wall parameters  $A_K$ . As the flexible substrate becomes a rigid substrate, the above result is fully consistent with the one obtained in Ref. [42].

In Fig. 6(a), a neutral curve in the  $k$ - $\mu$  plane is illustrated for various values of stiffness  $A_K$ , with all other parameters

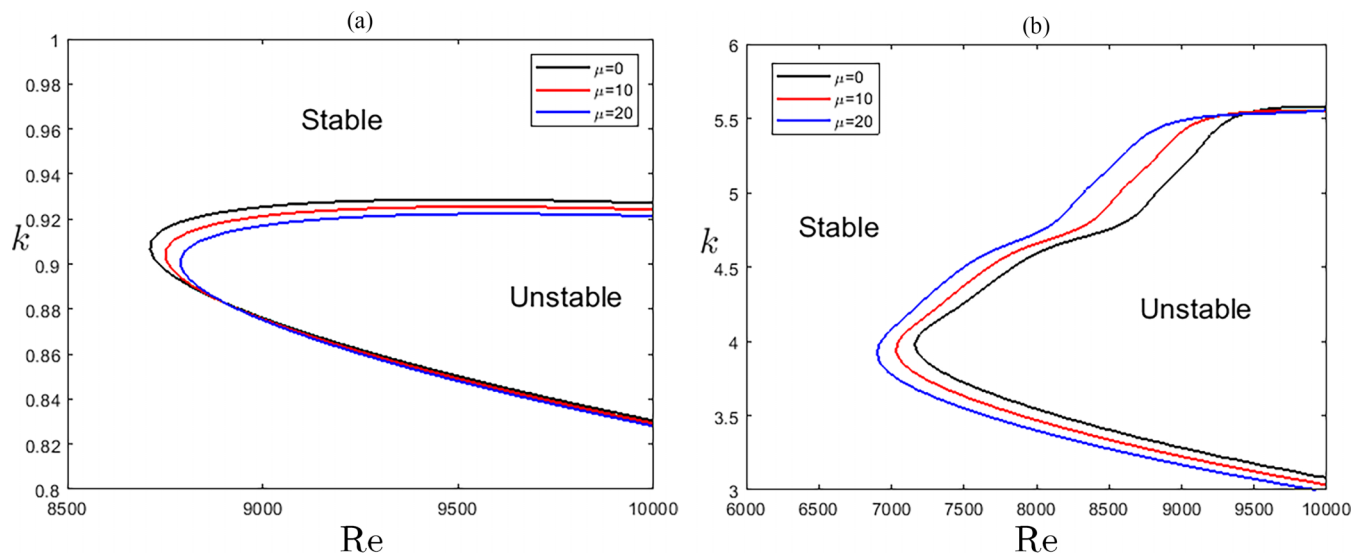


FIG. 7. (a) The neutral curve in the  $k$ - $Re$  plane with the different values of viscosity ratio  $\mu$  for shear mode, when  $A_I = A_T = A_B = 1$ ,  $A_K = 10\,000$ ,  $A_D = 10$ , and  $\alpha = \pi/180$ . (b) The neutral curve in the  $k$ - $\mu$  plane with the different values of viscosity ratio  $\mu$  for wall mode, when  $A_I = A_T = A_B = 1$ ,  $A_K = 10\,000$ ,  $A_D = 10$ , and  $\alpha = \pi/180$ .



set to unity. Figure 6(a) shows that the critical odd viscosity ratio  $\mu$  increases linearly with wave number when the stiffness coefficient  $A_K = 1$  and 3. There is another result at  $A_K = 8$  and 10 that has two branches for large  $\mu$ , in which the upper branch grows with  $\mu$  while the lower one decays as  $\mu$  increases. And we can find that the long wave instability should in turn disappear as the stiffness  $A_K$  is increased for the low values of Re. In Fig. 6(b), we observe a neutral curve in the  $k$ - $\mu$  plane for different inclination angles  $\alpha$ . It is indicated that the unstable region linearly extends for different values of  $\alpha$ , as the ratio of viscosity increases.

### C. Numerical results at high Reynolds number regime

According to the study of Floryan *et al.* [46], it is known that in falling film flows shear modes of instability enter in addition to the interfacial mode at higher Reynolds numbers and extremely small inclination angle  $\alpha$ . In addition, Alexander *et al.* [24] and Samanta [25] describe the wall mode in the high Reynolds numbers regime. Due to the complexity of parameters, we will briefly describe our results in the form of neutral stability curves in the  $k$ -Re plane. We choose the parameter values as  $A_K = 10^4$ ,  $\alpha = \pi/180$ , and others set to unity. Figure 7(a) demonstrates the neutral curve for the shear mode. It is observed that the unstable domain induced by the shear mode is reduced with the increasing value of odd viscosity coefficient  $\mu$ . It is the same as Samanta's conclusion [42], in which he studied the stability of a falling film of odd viscosity liquid on a rigid wall. Figure 7(b) displays that the unstable region generated by the wall mode is enlarged with the increasing value of the odd viscosity coefficient  $\mu$ . This means the instability of the wall mode is dominated by the characteristics of an elastic plate.

## V. CONCLUSION

This study systematically investigated the impacts of spontaneous odd viscosity, inertia, flexural rigidity, and spring stiffness of the flexible substrate on the stability of a falling liquid film. By taking into account the odd viscosity in the flexible wall model from Alexander *et al.* [24], we construct

the modified linear wall equation, which includes the odd viscosity effect. The OS equations can be obtained by combining the peculiar viscosity incompressible Navier-Stokes equations with the boundary conditions of the free interface. To analyze the stability of the arbitrary wave number, the Chebyshev collocation method is used to resolve the OS eigenvalue problem. We obtain the neutral curve in the  $k$ -Re plane and temporal growth rate  $\omega$  with the different values of odd viscosity rates  $\mu$ . The results in the moderate Reynolds number regime indicate that an increase in the viscosity ratio expands the unstable domain when the stiffness coefficient  $A_K$  is small. However, when the value of stiffness coefficient  $A_K$  enlarges, the effect of odd viscosity transforms to suppress the onset of instability. This implies that the effect of odd viscosity will convert when the flexible substrate behaves gradually as a rigid substrate with increasing values of the wall parameters  $A_K$ . The shear and wall modes of the instability are depicted respectively, at higher Reynolds numbers and extremely small inclination angle  $\alpha$ . The neutral curves in the  $k$ -Re plane for shear modes display the unstable domain is reduced by increasing the value of odd-viscosity coefficient  $\mu$ . And the opposite conclusion can be drawn in the wall modes.

The data used in this study are available from the corresponding author upon reasonable request.

## ACKNOWLEDGMENTS

Project supported by the National Natural Science Foundation of China (Grant No. 12262026), the Innovative Research Team in Universities of Inner Mongolia Autonomous Region (Grant No. NMGIRT2323), the Natural Science Foundation of Inner Mongolia Autonomous Region of China (Grant No. 2021MS01007), and the Inner Mongolia Grassland Talent (Grant No. 12000-12102013).

The authors declare that this manuscript is original, has not been published before, and is not currently being considered for publication elsewhere. The authors also declare that they have no known competing financial interests or personal relationships that could have appeared to influence the work reported in this paper.

- 
- [1] E. O. Tuck, *Phys. Fluids* **26**, 2352 (1983).
  - [2] S. J. Weinstein and K. J. Ruschak, *Annu. Rev. Fluid Mech.* **36**, 29 (2004).
  - [3] S. Zhao, M. Dietzel, and S. Hardt, *J. Fluid Mech.* **879**, 422 (2019).
  - [4] P. L. Kapitza, *J. Exp. Theor. Phys.* **19**, 105 (1949).
  - [5] A. M. Binne, *J. Fluid Mech.* **2**, 551(1957).
  - [6] T. B. Benjamin, *J. Fluid Mech.* **2**, 554(1957).
  - [7] C. S. Yih, *Phys. Fluids* **6**, 321(1963).
  - [8] R. E. Kelly, D. A. Goussis, S. P. Lin, and F. K. Hsu, *Phys. Fluids A* **1**, 819 (1989).
  - [9] M. K. Smith, *J. Fluid Mech.* **217**, 469(1990).
  - [10] S. J. D. D'Alessio, J. P. Pascal, E. Ellaban, and C. Ruyer-Quil, *J. Fluid Mech.* **887**, A20 (2020).
  - [11] M. M. Hossain, S. Ghosh, and H. Behera, *Phys. Fluids* **34**, 084111(2022).
  - [12] G. F. Dietze, *J. Fluid Mech.* **859**, 1098(2019).
  - [13] G. Lavalley, Y. Q. Li, S. Mergui, N. Grenier, and G. F. Dietze, *J. Fluid Mech.* **860**, 608 (2019).
  - [14] Z. Q. Zhou, J. Peng, Y. J. Zhang, and W. L. Zhuge, *J. Fluid Mech.* **802**, 583 (2016).
  - [15] M. O. Kramer, *J. Aero. Sci.* **24**, 459 (1957).
  - [16] T. B. Benjamin, *J. Fluid Mech.* **9**, 513 (1960).
  - [17] P. W. Carpenter and A. D. Garrad, *J. Fluid Mech.* **155**, 465 (1985).
  - [18] D. Halpern and J. B. Grotberg, *J. Fluid Mech.* **244**, 615 (1992).
  - [19] V. Gkanis and S. Kumar, *Phys. Fluids* **18**, 044103 (2006).
  - [20] V. Shankar and A. K. Sahu, *Phys. Rev. E* **73**, 016301 (2006).
  - [21] S. Sahu and V. Shankar, *Phys. Rev. E* **94**, 013111 (2016).
  - [22] S. Mandloi and V. Shankar, *Phys. Rev. E* **101**, 043107 (2020).
  - [23] Gaurav and V. Shankar, *Phys. Fluids* **22**, 094103 (2010).

- [24] J. P. Alexander, T. L. Kirk, and D. T. Papageorgiou, *J. Fluid Mech.* **900**, A40 (2020).
- [25] A. Samanta, *J. Fluid Mech.* **920**, A23 (2021).
- [26] S. Lebbal, F. Alizard, and B. Pier, *Phys. Rev. Fluids* **7**, 023903 (2022).
- [27] S. Lebbal, F. Alizard, and B. Pier, *J. Fluid Mech.* **948**, A15 (2022).
- [28] J. E. Avron, *J. Stat. Phys.* **92**, 543(1998).
- [29] M. F. Lapa and T. L. Hughes, *Phys. Rev. E* **89**, 043019 (2014).
- [30] S. Ganeshan and A. G. Abanov, *Phys. Rev. Fluids* **2**, 094101 (2017).
- [31] A. Abanov, T. Can, and S. Ganeshan, *SciPost Phys.* **5**, 010 (2018).
- [32] D. Banerjee, A. Souslov, A. G. Abanov, and V. Vitelli, *Nat. Commun.* **8**, 1573 (2017).
- [33] J. C. Tsai, F. Ye, J. Rodriguez, J. P. Gollub, and T. C. Lubensky, *Phys. Rev. Lett.* **94**, 214301 (2005).
- [34] Y. Sumino, K. H. Nagai, Y. Shitaka, D. Tanaka, K. Yoshikawa, H. Chat, and K. Oiwa, *Nature (London)* **483**, 448 (2012).
- [35] C. Maggi, F. Saglimbeni, M. Dipalo, F. De Angelis, and R. Di Leonardo, *Nat. Commun.* **6**, 7855 (2015).
- [36] E. Kirkinis and A. V. Andreev, *J. Fluid Mech.* **878**, 169 (2019).
- [37] V. Soni, E. S. Billign, S. Magkiriadou, S. Sacanna, D. Bartolo, M. J. Shelley, and W. T. M. Irvine, *Nat. Phys.* **15**, 1188 (2019).
- [38] G. Bao and Y. Jian, *Phys. Rev. E* **103**, 013104 (2021).
- [39] J. Zhao and Y. Jian, *Fluid Dyn. Res.* **53**, 015510 (2021).
- [40] J. Zhao and Y. Jian, *Phys. Scr.* **96**, 055214 (2021).
- [41] B. N. Jia and Y. J. Jian, *Phys. Fluids* **34**, 044104 (2022).
- [42] A. Samanta, *J. Fluid Mech.* **938**, A9 (2022).
- [43] X. Chu, L. Chang, B. N. Jia, and Y. J. Jian, *Phys. Fluids* **34**, 114123 (2022).
- [44] S. Chattopadhyay, A. S. Desai, A. K. Gaonkar, and A. Mukhopadhyay, *Phys. Rev. Fluids* **8**, 064003 (2023).
- [45] Y. Y. Han, J. Y. Li, and F. F. Qing, *Phys. Fluids* **28**, 102101 (2016).
- [46] J. M. Floryan, S. H. Davis, and R. E. Kelly, *Phys. Fluids* **30**, 983 (1987).